

# Computational Studies of Transition Metal Nanoalloys

Bearbeitet von  
Lauro Oliver Paz Borbón

1. Auflage 2013. Taschenbuch. xvi, 156 S. Paperback

ISBN 978 3 642 26762 8

Format (B x L): 15,5 x 23,5 cm

Gewicht: 272 g

Weitere Fachgebiete > Chemie, Biowissenschaften, Agrarwissenschaften >  
Physikalische Chemie > Quantenchemie, Theoretische Chemie

Zu [Inhaltsverzeichnis](#)

schnell und portofrei erhältlich bei

The logo for beck-shop.de features the text 'beck-shop.de' in a bold, red, sans-serif font. Above the 'i' in 'shop' are three red dots of varying sizes, arranged in a slight arc. Below the main text, the words 'DIE FACHBUCHHANDLUNG' are written in a smaller, red, all-caps, sans-serif font.

**beck-shop.de**  
DIE FACHBUCHHANDLUNG

Die Online-Fachbuchhandlung [beck-shop.de](http://beck-shop.de) ist spezialisiert auf Fachbücher, insbesondere Recht, Steuern und Wirtschaft. Im Sortiment finden Sie alle Medien (Bücher, Zeitschriften, CDs, eBooks, etc.) aller Verlage. Ergänzt wird das Programm durch Services wie Neuerscheinungsdienst oder Zusammenstellungen von Büchern zu Sonderpreisen. Der Shop führt mehr als 8 Millionen Produkte.

## Chapter 2

# Theoretical Background and Methodology

In this chapter the different approaches followed in order to model metal nanoparticles are described. The theoretical framework adopted in this work, varying from the use of an empirical potential (i.e. the Gupta potential) to ab initio methods such as density functional theory (DFT) is explained. An introduction to different global optimization techniques, for the exploration of the nanoparticle potential energy surface, as well as a combined Gupta-DFT approach is also given. Finally, energetic quantities for analysing the stability of nanoparticles are described in detail.

### 2.1 Modelling Metal Clusters and Nanoalloys

Different approaches can be used to model atom–atom interactions in metal clusters and nanoalloys, and to search for putative stable configurations, i.e. to locate the global minimum (GM) on the nanoparticle potential energy surface (PES). This is a very difficult task because the properties of each system will depend on its constituent elements and size. The complexity will also depend on how accurate the model we are using is, ranging from: pair-wise potentials (such as the Lennard–Jones potential; an approximation which is quite accurate for noble gases, in which the interatomic interactions depend mainly on the distances between atoms); and many-body potentials (e.g. the Gupta potential, Embedded Atom and Sutton–Chen potentials); to computationally intensive *first-principle* methodologies (e.g. Hartree–Fock calculations, DFT, or more expensive post-Hartree–Fock methods such as configuration interaction (CI) or Møller–Plesset perturbation theory). Pair-wise potentials are simple approximations for describing atomic interactions, in which the nature of the interactions depends on attractive and repulsive terms (having parameters, fitted either to experimental observations or calculated theoretically); and where the total

energy of the system can be calculated in terms of the atomic positions ( $r_1, r_2, \dots, r_N$ ). Many-body potentials, such as Gupta, tend to overcome the high computational cost/effort of first principles calculations while keeping the many-body nature of metallic bonding. When coupled with global optimization tools (e.g. Genetic algorithms and Basin Hopping Monte Carlo algorithms) this allows us to explore large areas of the nanoparticle PES in a feasible amount of time, while at the same time, accurately simulating the interatomic interactions.

### 2.1.1 Potential Energy Surfaces

One of the main goals in this study is to determine the global minimum (GM) structure (i.e. the structural configuration with the lowest total potential energy) for a metal cluster of a certain size and elemental composition. It is known that experimental information is not always sufficient for determining the nanocluster structure precisely and theoretical predictions are of great importance in this field. Understanding the structural configuration of nanoclusters (as well as their energetics) will aid the tailored design of nanoparticles, in which the nanoparticle's physical and chemical properties can be fine tuned. The potential energy of a nanoparticle ( $V_{\text{clus}}$ ), can be represented on a potential energy surface (PES) diagram. The PES of a system is represented in terms of the atomic coordinates. The number of interacting atoms in the system ( $N$ ) leads to  $3N$  degrees of freedom, yielding a PES dimensionality of  $3N + 1$ , where the extra dimension is the potential energy.

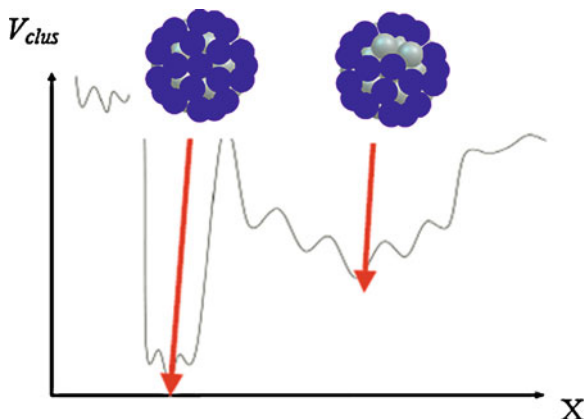
A local minimum in the PES is defined as a point, in which any displacement will lead to higher potential energy ( $V_{\text{clus}}$ ) configurations. The gradients at this point are all zero,  $\nabla V_{\text{clus}} = 0$ , and all the curvatures (second derivatives) are positive. The PES of a small system can have large numbers of *local-minima*, which correspond to high-energy arrangements. The lowest energy configuration is called the *global-minimum* (GM) [1]. Figure 2.1 shows a schematic representation of two systems of fixed size and composition, but having differ segregation patterns between A (blue) and B (grey) metals. One can see that a particular chemical ordering in the nanoparticle will lead to a lower energy configuration (a more stable structure).

## 2.2 Theoretical Methods

### 2.2.1 The Gupta Potential

The Gupta potential [2, 3] is based on the second moment approximation to Tight Binding theory. It is written in terms of repulsive ( $V^r$ ) pair and attractive many-body ( $V^m$ ) terms, which are obtained by summing over all ( $N$ ) atoms:

**Fig. 2.1** Pictorial representation of a potential energy surface of two bimetallic cluster homotops, having the same number of atoms A (grey) and B (blue) and geometries. They occupy different regions in the PES (different *basins*), due to differences in *chemical ordering*



$$V_{\text{clus}} = \sum_i^N \{V^r(i) - V^m(i)\} \quad (2.1)$$

where:

$$V^r(i) = A(a, b) \sum_{j \neq i}^N \exp\left(-p(a, b) \left(\frac{r_{ij}}{r_0(a, b)} - 1\right)\right) \quad (2.2)$$

and

$$V^m(i) = \zeta(a, b) \sqrt{\sum_{j \neq i}^N \exp\left(-2q(a, b) \left(\frac{r_{ij}}{r_0(a, b)} - 1\right)\right)} \quad (2.3)$$

In Eqs. 2.2 and 2.3,  $r_{ij}$  represents the interatomic distance between atoms  $i$  and  $j$ .  $A$ ,  $r_0$ ,  $\zeta$ ,  $p$  and  $q$  are fitted to experimental values of the cohesive energy, lattice parameters and independent elastic constants for crystal structures of pure metals and bulk alloys and  $a$  and  $b$  define the element types of atoms  $i$  and  $j$ , respectively. Gupta potential parameters used in this research are listed in Table 2.1. For the discussion of varying Pd–Pt parameters and two different fitted Pd–Au parameter sets, see Chaps. 6 and 7, respectively.

### 2.2.2 Early Density Functional Theory: Thomas Fermi Model

A first approximation to studies at the atomic level was made using Newtonian mechanics and classical electromagnetism. Due to the failure to explain the structure and complexity of atomic systems, new theories had to be proposed. Thomas and Fermi gave the first formal derivation of a density functional approach for a system

**Table 2.1** Gupta potential parameters used in this research [3]

Parameters	Pd–Pd	Pt–Pt	Ag–Ag	Au–Au	Au–Au (for Ag–Au)	Ag–Au	Ag–Pt	Pd–Au	Pd–Pt
$A$ (eV)	0.1746	0.2975	0.1031	0.2061	0.2096	0.1488	0.175	0.19	0.23
$\zeta$ (eV)	1.718	2.695	1.1895	1.790	1.8153	1.4874	1.79	1.75	2.2
$p$	10.867	10.612	10.85	10.229	10.139	10.494	10.73	10.54	10.74
$q$	3.742	4.004	3.18	4.036	4.033	3.607	3.57	3.89	3.87
$r_0$ (Å)	2.7485	2.7747	2.8921	2.884	2.885	2.8885	2.833	2.816	2.76

of electrons in an external potential, due to nuclei [4, 5]. In their model the total energy of an inhomogeneous electron gas is written as a functional of the electronic density,  $\rho(\vec{r})$ . This was an initial (rough) approximation to the exact solution of the many-electron Schrödinger equation and the associated wave function  $\Psi(r_1, r_2, \dots, r_N)$ , and is the most primitive version of DFT.

$$E_{\text{TF}}[\rho(\vec{r})] = T_{\text{TF}}[\rho(\vec{r})] + E_{\text{en}}[\rho(\vec{r})] + E_{\text{ee}}[\rho(\vec{r})] \quad (2.4)$$

In the Thomas–Fermi (TF) model, the electronic density  $\rho(\vec{r})$  completely characterizes the ground state of the system. As the TF model neglects exchange (included in the Hartree–Fock method, as a consequence of the anti-symmetry of the wave function, i.e. the Pauli exclusion principle) and correlation effects; the energy functional  $E_{\text{TF}}[\rho(\vec{r})]$  is expressed as the contribution of kinetic energy ( $T_{\text{TF}}[\rho(\vec{r})]$ ), the electron–nucleus attraction ( $E_{\text{en}}[\rho(\vec{r})]$ ) and electron–electron repulsion ( $E_{\text{ee}}[\rho(\vec{r})]$ ). In the TF model, the kinetic energy is expressed as a functional of the electronic density  $\rho(\vec{r})$ .

$$T_{\text{TF}}[\rho(\vec{r})] = C_{\text{F}} \int \rho^{5/3}(\vec{r}) d\vec{r} \quad (2.5)$$

hence, the energy functional can be written as follows:

$$E_{\text{TF}}[\rho(\vec{r})] = C_{\text{F}} \int \rho^{5/3}(\vec{r}) d\vec{r} - Z \int \frac{\rho(\vec{r})}{r} d\vec{r} + \frac{1}{2} \int \int \frac{\rho(\vec{r})\rho(\vec{r}')}{|\vec{r} - \vec{r}'|} d\vec{r} d\vec{r}' \quad (2.6)$$

with  $C_{\text{F}} = \frac{3}{10}(3\pi^2)^{2/3} = 2.871$ ; calculated from the jellium model. The TF model assumes that the electronic density  $\rho(\vec{r})$  minimizes the energy functional  $E_{\text{TF}}[\rho(\vec{r})]$ , with the constraint:

$$N = N[\rho(\vec{r})] = \int \rho(\vec{r}) d\vec{r} \quad (2.7)$$

where integrating over  $\rho(\vec{r})$ , gives the total number of electrons,  $N$ . Using the Lagrange multipliers method in order to find a stationary point for  $E[\rho(\vec{r})]$ , using the constraint 2.7:

$$\frac{\delta}{\delta\rho(\vec{r})} \left[ E_{\text{TF}}[\rho(\vec{r})] - \mu_{\text{TF}} \left( \int \rho(\vec{r}) d\vec{r} - N \right) \right] = 0 \quad (2.8)$$

the variations in electronic density of the energy functional  $E_{\text{TF}}[\rho(\vec{r})]$ , can be expressed as an Euler–Lagrange equation, where:

$$\frac{\delta E_{\text{TF}}[\rho(\vec{r})]}{\delta \rho(\vec{r})} = \mu_{\text{TF}} \quad (2.9)$$

$$\mu_{\text{TF}} = \frac{\delta E_{\text{TF}}[\rho(\vec{r})]}{\delta \rho(\vec{r})} = \frac{5}{3} C_{\text{F}} \rho^{2/3}(\vec{r}) - \phi(\vec{r}) \quad (2.10)$$

where  $\phi(\vec{r})$ :

$$\phi(\vec{r}) = \frac{Z}{r} - \int \frac{\rho(\vec{r}')}{|\vec{r} - \vec{r}'|} d\vec{r}' \quad (2.11)$$

Equation 2.11 can be solved using the density constraint (Eq. 2.7), and the resulting density is then inserted in Eq. 2.6, in order to give the total energy of the system. The TF model is a very simple theory for describing total energies of atoms, which set up the foundations for a more complex DFT [6, 7].

### 2.2.3 Modern Density Functional Theory

For the case of  $N$  interacting electrons (in the ground-state), their interactions can be described as the sum of the kinetic energy ( $\hat{T}$ ), external potential ( $\hat{V}$ ) and Coulombic ( $\hat{V}_{\text{ee}}$ ) operators. The corresponding Hamiltonian operator ( $\hat{H}$ ):

$$\hat{H} = \hat{T} + \hat{V} + \hat{V}_{\text{ee}} \quad (2.12)$$

which can be expressed, in a similar way, in the following analytic form:

$$\hat{H} = - \sum_{i=1}^N \frac{1}{2} \nabla_i^2 + \sum_{i=1}^N v(\vec{r}_i) + \frac{1}{2} \sum_{i=1}^N \sum_{i \neq j}^N \frac{1}{|\vec{r}_i - \vec{r}_j|}$$

where  $v(\vec{r}_i)$  represents the external potential. The Hamiltonian  $\hat{H}$ , described in the equation above, takes into account the adiabatic Born–Oppenheimer approximation. The Born–Oppenheimer approximation treats the atomic nucleus as being fixed in position, with respect to the electronic motion, due to large mass differences between the atomic nucleus and the electron. This represents a decoupling of the motion of the electrons and the motion of the nucleus; hence one needs to solve the Schrödinger equation only for the electronic part [8].

The foundations of modern DFT were published in the classic papers of Hohenberg and Kohn in 1964, and Kohn and Sham one year later [9, 10]. They developed an exact variational principle formalism in which ground state properties, such as: total electronic energy, equilibrium positions and magnetic

moments are expressed in terms of the total electronic density  $\rho(\vec{r})$ . The theorems are explained below:

Hohenberg and Kohn Theorem: the ground state density  $\rho(\vec{r})$  of a bound system of interacting electrons in some external potential  $v(\vec{r})$  determines this potential uniquely, as well as the ground state wave-function  $\Psi(r_1, \dots, r_N)$ .

This theorem also states that: since electronic density  $\rho(\vec{r})$  determines both the total number of electrons,  $N$  and the external potential  $v(\vec{r})$ ;  $\rho(\vec{r})$  also provides a full description of all the ground-state observables, which are functionals of  $\rho(\vec{r})$  [11]. Another statement of the Hohenberg–Kohn theorem states: the ground state energy  $E_0$  and the ground-state density  $\rho_0(\vec{r})$  of a system characterized by an external potential  $v(\vec{r})$  can be obtained by using the variational principle (involving only the density).

In other words, the ground state energy  $E_0$  can be expressed as a functional of the ground state density  $E_v[\rho(\vec{r})]$ , otherwise the inequality prevails [6]:

$$E_0 = E_v[\rho_0(\vec{r})] < E_v[\rho(\vec{r})] \quad (2.14)$$

The theory also established the existence of a universal functional,  $F[\rho(\vec{r})]$  which is independent of the external potential  $v(\vec{r})$ , i.e. which has the same functional form for any system considered. The universal functional  $F[\rho(\vec{r})]$ , can be expressed as the sum of the kinetic energy of the gas of non-interacting Kohn–Sham electrons ( $T_s[\rho(\vec{r})]$ ), the Coulombic electron–electron interaction, and the exchange-correlation term ( $E_{xc}[\rho(\vec{r})]$ ) as follows:

$$F[\rho(\vec{r})] = T_s[\rho(\vec{r})] + \frac{1}{2} \int \int \frac{\rho(\vec{r})\rho(\vec{r}')}{|\vec{r} - \vec{r}'|} + E_{xc}[\rho(\vec{r})] \quad (2.15)$$

The  $E_{xc}[\rho(\vec{r})]$  term is expressed as the sum of the correlation ( $E_c[\rho(\vec{r})]$ ) and the exchange energy ( $E_x[\rho(\vec{r})]$ ). In the  $E_{xc}[\rho(\vec{r})]$  term, the correlation energy  $E_c[\rho(\vec{r})]$  is expressed as the difference between the true kinetic energy  $T[\rho(\vec{r})]$  and  $T_s[\rho(\vec{r})]$ :

$$E_c[\rho(\vec{r})] = T[\rho(\vec{r})] - T_s[\rho(\vec{r})] \quad (2.16)$$

The exchange  $E_x[\rho(\vec{r})]$  term is derived from Hartree–Fock Theory (Slater determinant). The Slater determinant, which takes into account the antisymmetry of the wavefunction from the Pauli exclusion principle (i.e. an electron having either spin  $\alpha$  or spin  $\beta$ ) assures a change of sign under electron exchange:

$$\begin{aligned} & \psi(\vec{r}_1, \vec{r}_2, \dots, \vec{r}_N) \\ &= \sqrt{\frac{1}{N!}} \begin{vmatrix} \phi_0(\vec{r}_1)\alpha(s_1) & \phi_0(\vec{r}_2)\beta(s_1) & \dots & \phi_{N/2-1}(\vec{r}_1)\alpha(s_1) & \phi_{N/2-1}(\vec{r}_1)\beta(s_1) \\ \dots & \dots & \dots & \dots & \dots \\ \phi_0(\vec{r}_N)\alpha(s_N) & \phi_0(\vec{r}_N)\beta(s_N) & \dots & \phi_{N/2-1}(\vec{r}_N)\alpha(s_N) & \phi_{N/2-1}(\vec{r}_N)\beta(s_N) \end{vmatrix} \end{aligned} \quad (2.17)$$

Therefore, the total energy of a system ( $E_v[\rho(\vec{r})]$ ), under a external potential,  $v(\vec{r})$ , can be expressed as:

$$E_v[\rho(\vec{r})] = F[\rho(\vec{r})] + \int \rho(\vec{r})v(\vec{r})d^3\vec{r} \quad (2.18)$$

Using the variational principle with the constraint 2.7 the ground state density satisfies the stationary principle:

$$\delta \left[ E_v[\rho(\vec{r})] - \mu \left( \int \rho(\vec{r})d^3\vec{r} - N \right) \right] = 0 \quad (2.19)$$

which gives the Euler–Lagrange equation:

$$\frac{\delta E_v[\rho(\vec{r})]}{\delta \rho(\vec{r})} = v(\vec{r}) + \frac{\delta F[\rho(\vec{r})]}{\delta \rho(\vec{r})} \quad (2.20)$$

From the Hohenberg–Kohn theorems, we have derived the Kohn–Sham (KS) equations [6, 7, 10]. The KS equations solve the problem of the complex many-electron Schrödinger equations, by transforming them into a set of  $N$  single-electron equations, which need to be solved self-consistently.

$$\left[ -\frac{1}{2}\nabla^2 + v(\vec{r}) + \int \frac{\rho(\vec{r}')}{|\vec{r} - \vec{r}'|} d^3\vec{r}' + v_{xc}[n(\vec{r})] \right] \psi_i(\vec{r}) = \epsilon_i \psi_i(\vec{r}) \quad (2.21)$$

with an electronic density:

$$\rho(\vec{r}) = \sum_{i=1}^N |\psi_i(\vec{r})|^2 \quad (2.22)$$

In Eq. 2.21, the exchange-correlation potential,  $v_{xc}[n(\vec{r})]$  is expressed as the partial derivative of the  $E_{xc}[\rho(\vec{r})]$  term, with respect to the electronic density,  $\rho(\vec{r})$ :

$$\frac{\delta E_{xc}[\rho(\vec{r})]}{\delta \rho(\vec{r})} = v_{xc}[\rho(\vec{r})] \quad (2.23)$$

This means we have to start from some initial electronic density ( $\rho_0(\vec{r})$ ) and proceed to solve Eq. 2.21. We obtain a new density which is used to solve Eq. 2.21 until self-consistency is reached [6, 7, 11]. DFT does not provide a description of how to construct the exchange-correlation functional,  $E_{xc}[\rho(\vec{r})]$ , it only stipulates the existence of  $E_{xc}[\rho(\vec{r})]$  as a universal functional of the density  $\rho(\vec{r})$ , which is valid for all systems. Several approximations have been constructed (for the accurate description of the exchange-correlation energy,  $e_{xc}^{\text{inif}}[\rho(\vec{r})]$ ), such as the *local-density approximation* (LDA) [11]. This formulation is established in the original Kohn–Sham theory, and the idea is that a system with inhomogeneous charge distribution is treated as having a *locally-homogeneous* spatial uniform distribution of  $\rho(\vec{r})$ :

$$E_{xc}^{\text{LDA}}[\rho(\vec{r})] = \int \rho(\vec{r})e_{xc}^{\text{unif}}[\rho(\vec{r})]d^3\vec{r} \quad (2.24)$$

where an approximate analytical expression for  $e_{xc}^{\text{unif}}[\rho(\vec{r})]$  comes from the  $e_x$  Hartree–Fock exchange term (Slater determinant), and  $e_c$  is fitted from quantum Monte Carlo parametrizations of homogeneous electron gases of varying densities [12]. LDA offers a good level of accuracy for highly-homogeneous systems, and even for realistic non-homogeneous systems; while one of the drawbacks is its overestimation of binding energies for molecules and solids [11, 13]. Some other high-level approximations to the  $e_{xc}^{\text{unif}}[\rho(\vec{r})]$  have been made, such as the *generalized gradient approximation* (GGA) [11, 14, 15], for which the exchange-correlation energy (for a spin-unpolarized system) is expressed as:

$$E_{xc}^{\text{GGA}}[\rho(\vec{r})] = \int f[\rho(\vec{r}), \nabla\rho(\vec{r})] d^3\vec{r} \quad (2.25)$$

in which the density  $\rho(\vec{r})$  is expanded in terms of the gradient ( $\nabla$ ) operator. This approximation is valid for systems with slowly-varying densities.

In order to solve the Kohn–Sham equations, we need to select a suitable (sufficiently large) finite basis set (in theory one will need an infinite basis set for a precise description of the molecular orbital). We can express the wave-function  $\psi$  in terms of Gaussian-type-orbitals (GTOs), in either cartesian or polar coordinates:

$$\psi(\vec{r}) = Ax^lx^ly^ly^lz^lz \exp(-\zeta r^2) \quad (2.26)$$

where  $A$  is a normalization constant,  $l$  determines the orbital,  $\zeta$  is related to the width of the curve, and the  $r^2$  gives the curve a Gaussian shape [16].

## 2.2.4 Functionals and Basis Sets

DFT calculations were performed using the **NWChem** (versions 4.7, 5.0 and 5.1) quantum chemistry package [17] and the Perdew–Wang exchange-correlation functional (PW91) [14, 15]. Test calculations using the Perdew–Burke–Ernzerhof (PBE) gradient-corrected exchange-correlation functional [18] produced qualitatively similar results while hybrid functionals (such as B3LYP) tend to underestimate atomization energies of  $d$ -metals, due to the inclusion of the Hartree–Fock exchange term, and its lack of a proper description of the nearly “free-electron” character of large metallic systems [19, 20].

Spherical Gaussian-type-orbital basis sets of double- $\zeta$  quality [21, 22] were used for Pd ( $7s6p5d$ )/[ $5s3p2d$ ], Ag ( $7s6p5d$ )/[ $5s3p2d$ ], Pt ( $7s6p5d$ )/[ $6s3p2d$ ] and Au ( $7s5p5d$ )/[ $6s3p2d$ ]; combined with effective core potentials (ECP) in order to consider valence–electron only wavefunctions: 18 valence electrons were considered for Pd and Pt while 19 valence electrons were used for Ag and Au [23]. The ECP incorporates spin–orbit averaged relativistic for these four atoms.

Charge density fitting basis sets were used to speed up the evaluation of the Coulombic contributions [24]: Pd ( $8s7p6d5f4g$ )/[ $8s6p6d3f2g$ ], Ag ( $9s4p5d3f4g$ )/[ $7s4p4d3f2g$ ], Pt ( $9s4p3d3f4g$ )/[ $9s4p3d3f2g$ ], and Au ( $9s4p4d3f4g$ )/[ $8s4p3d3f2g$ ].

All calculations were performed spin unrestricted (geometry optimization for singlet spin states; after SCF optimization convergence a single point triplet spin state calculation is performed). Geometry optimizations were stopped when maximum force on atoms was less than  $4 \times 10^{-4}$  a.u. During the iterative process, a Gaussian smearing technique was adopted, with a smearing parameter of 0.136 eV for the fractional occupation of the one-electron energy levels [25]. Selected calculations were performed with basis sets of triple- $\zeta$ -plus-polarization quality to evaluate DFT mixing energies for comparison with Gupta values [21, 22].

For the fitting of the DFT-fit parameters for Pd–Au (see Chap. 7), DFT calculations on the solid phases were performed using the **PWscf** (Plane-Wave self-consistent-field) computational code [26], employing ultra-softpseudo-potentials (Dr. Giovanni Barcaro, CNR-Pisa). A total of 10 and 11 electrons were explicitly considered for Pd and Au, respectively. The PBE gradient-corrected exchange-correlation functional was used. Values of 40 Ry for the energy cutoff of the wave function and 160 Ry for the energy cutoff (1 Ry = 13.606 eV) of the electronic density have been shown to provide accurate results [as shown in previous work for the description of a monolayer phase of TiO<sub>x</sub> on Pt(111)], and were thus employed [27]. All the calculations were performed by applying a smearing procedure of the energy levels with a Gaussian broadening of 0.002 Ry. The Brillouin zone was described by a  $(10 \times 10 \times 10)$  grid.

## 2.3 Global Optimization Techniques

### 2.3.1 *The Birmingham Cluster Genetic Algorithm*

Genetic algorithms (GA) were developed by John Holland in the early 1970s, and since then, they have become successful tools in optimization problems in fields such as: chemistry, engineering and molecular modelling [28–30]. GAs belong to the class of stochastic optimization methods, which also includes techniques such as: evolutionary strategies, simulated annealing, and Monte Carlo optimization.

Structural global optimisation of a model potential function, consists of finding the configuration for which the PES is an absolute minimum: i.e. the GM. In recent years, GA techniques have been shown to be robust for finding the GM for a variety of types of nanoclusters [30, 31]. In a general way, genetic algorithms begin with an initial population of candidate solutions (in our studies, an initial population of starting cluster structures), which, through several iterative steps in the algorithm (crossover, mutation and natural selection), evolve towards the best solution of the problem (i.e the GM in the PES).

Our in-house Birmingham cluster genetic algorithm (BCGA) was written in order to find GM structures for several metallic and bimetallic systems, using the Gupta potential to model their interatomic interactions [30]. Its specific features and operators are defined as follows:

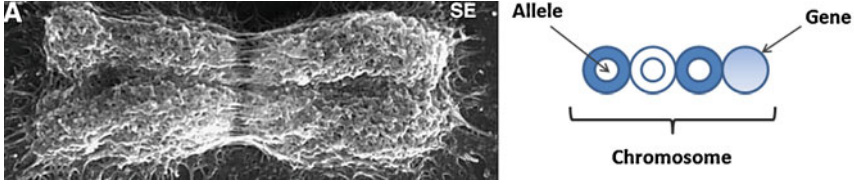


**Fig. 2.2** *Left* field emission scanning electron microscopy image of a barley chromosome metaphase. *Right* schematic representation of the cluster information encoding in a string (*chromosome*) in the GA code [32]

*Initial population* the group of individuals which are going to be evolved by the genetic algorithm. In the BCGA, the initial population corresponds to a set of randomly generated clusters; where real valued Cartesian coordinates are generated within a cubic volume which is proportional to the number of atoms within the cluster. This initial population is then relaxed using a quasi-Newton (L-BFGS) minimization routine [33]. When we talk about individuals, we refer to a set of variables, known as *genes*. Genes form strings called *chromosomes*, which represent a trial solution of the problem. Individual *gene* values are known as *alleles*. Figure 2.2 shows a Field emission scanning electron microscopy image which illustrates a barley chromosome metaphase along with the simplified *chromosome* version implemented in the BCGA [32].

*Fitness* is defined (for a member of a certain population) as the quality of the trial solution represented by a *chromosome*, with respect to the function being optimized. In our GA optimizations, high values correspond to a better solution to the problem. In the BCGA, the total potential energy ( $V_i$ ) of a cluster is first rescaled (Eq. 2.27), relative to the highest ( $V_{\max}$ ) and lowest ( $V_{\min}$ ) energy cluster in the current population:

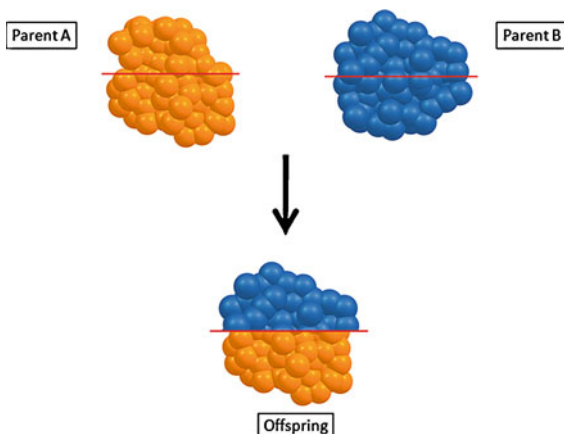
$$\rho_i = \frac{V_i - V_{\min}}{V_{\max} - V_{\min}} \quad (2.27)$$

A *fitness* function ( $F_i$ ), Eq. 2.28, is used by the BCGA in order to determine, according to a probabilistic value (in which 0 is the worst option and 1 the best one) which individuals will survive from one generation to the next.

$$F_i = \frac{1}{2} [1 - \tanh(2\rho_i - 1)] \quad (2.28)$$

*Selection of parents for crossover* in the BCGA, individuals are selected to take part in the crossover based on their *fitness*. There are different methodologies, such as: (a) *roulette wheel selection*, in which a string is chosen at random, and selected for crossover if its *fitness* value is greater than a random number generated between 0 and 1; and (b) *tournament selection*, in which a number of *strings* are randomly selected from the population. The two highest *fitness strings* are then selected as parents from this tournament pool.

**Fig. 2.3** Schematic representation of GA crossover



*Crossover* also known as “mating”, is the exchange of genetic information between *chromosomes* (*string* parents). In the BCGA, parent structures are combined in order to generate *offspring*, by the cut-and-splice procedure of Deavon and Ho [30]. In our work, we have used the 1-point-weighted *crossover* (see Fig. 2.3), in which the cut position is based on the energies of the parents (the relative *fitness* of the parents). The BCGA slices the two clusters parent and combines complementary slices, with more atoms being chosen from the parent of highest fitness. In our implementation, only one offspring is generated.

*Mutation* as in nature, mutations help to avoid stagnation of the population (i.e. they increase population diversity). Mutations results in slight changes in the genetic information encoded in the *chromosome*: in other words, new genetic material is introduced into the *population*. In global optimization routines, introducing a mutation operator can help to avoid convergence to a non-optimal solution (a high-energy nanocluster structure). In the BCGA, a number of different mutation schemes have been encoded:

- (a) *Replacement* one cluster is removed from the population and replaced by another generated at random.
- (b) *Rotation* a rotation of the atomic coordinates is performed of the top half of the cluster relative to the bottom half, by a random angle.
- (c) *Exchange* applied to bimetallic clusters, in which approximately one-third of the *A* type atoms in the cluster are exchanged for *B* atoms, without altering the original coordinates in the cluster
- (d) *Displacement* approximately one-third of the atoms in the clusters are displaced to random positions. The selected atoms are also chosen at random.

*Selection* evolutionary principles are best applied at this stage during GA searches (i.e. the Darwinian principle of survival of the “fittest”). There are modifications which can be taken into account, such as accepting all mutant structures (or the contrary case), not accepting parents for the next generation, or always keeping among the population the individuals with higher *fitness* (i.e. the elitist strategy).

*Optimization* all processes, such as crossover, mutation and selection is repeated for a specified number of generations (in this work, number of generations = 400) until the population is considered to be converged (when the range of cluster energies in the population has not changed for a prescribed number of generations).

The *BCGA parameters* adopted in this work were: population size = 40 clusters; crossover rate = 0.8 (i.e. 32 offspring are produced per generation); crossover type = 1-point weighted; selection = roulette; mutation rate = 0.1; mutation type = mutate-move; number of generations = 400, and number of GA runs for each composition = 100 (for statistical purposes, as well as for large clusters, a large number of global optimization searches are needed due to the complexity of the PES of the nanoparticle). Most of the parameters are selected as default by the BCGA code (such as crossover and mutation rate). A large initial population and a vast number of generations are needed for a full exploration of the PES of these medium size clusters. BCGA global optimizations were stopped when there is no change in the population over 10 different generations (term = 10).

### 2.3.2 The Basin-Hopping Monte Carlo Algorithm

A more detailed homotop search was performed using a modified version of the Basin Hopping Monte-Carlo algorithm (BHMC) [34], which allows only “atom-exchange” for a fixed composition and structural configuration (see Fig. 2.4).

During our local BHMC optimizations, we carried out approximately 3,000 Monte-Carlo steps, with a thermal energy  $k_B T$  of 0.02 eV. This low value is appropriate for performing a localized search of deep regions of the chosen structural funnel in the PES. We found that in some cases, the GA approach was not able to identify the most favorable chemical ordering, whereas this was easily found using the BHMC algorithm. This is in line with recent observations that the optimal strategy in configurational searches is to take initially only structural moves, and subsequently to refine the lowest-energy structures via atom-exchange moves [35, 36 and Ferrando and Rossi (2007, personal communication)].

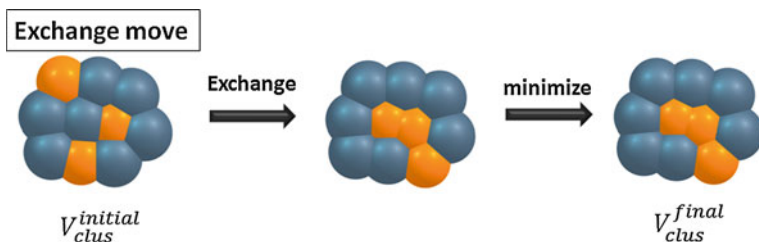
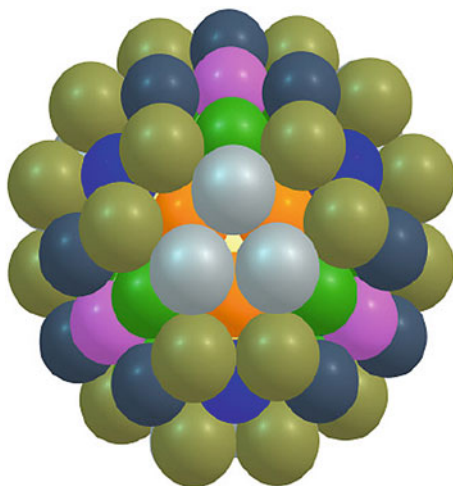


**Fig. 2.4** Schematic representation of the “atom-exchange” local relaxation, implemented in the BHMC algorithm

**Fig. 2.5** 98-atom Leary Tetrahedron (LT) structure with  $T_d$  symmetry. Each colour represents a different atomic shell



### 2.3.3 Shell Optimization Routine

For high-symmetry polyhedral cluster geometries, a substantial reduction in the search space is obtained if all sets of symmetry-equivalent atoms, which we have termed *atomic shells*, in a particular structure are constrained to be of the same chemical species [37]. It should be noted that these *atomic shells* are, in a more rigorous group theoretical sense, known as *orbits* of the point group [1]. For a given geometrical structure, this reduces the number of inequivalent compositional and permutational isomers (homotops) to  $2^S$ , where  $S$  is the number of atomic shells.

We have used our *shell optimization routine* for the highly symmetric 98-atom Leary tetrahedron (LT) structures (see Chaps. 4, 7), with ideal  $T_d$  symmetry.  $S = 9$  shells and, in order of increasing distance from the centre of the cluster, these shells have 4:12:12:12:4:6:12:12:24 atoms, resulting in  $2^9 = 512$   $T_d$  symmetry LT isomers. The various shells of the LT structure are indicated in Fig. 2.5 by different colours. Using the *shell-optimization routine*, it is possible to conduct a systematic investigation of all high-symmetry chemical arrangements for a given structural motif, with greatly reduced computational effort.

### 2.3.4 Combined EP-DFT Approach

In this work, we have followed a *combined approach* (see Fig. 2.6), in which initial global optimizations are carried out using our GA (coupled with the Gupta potential) and once we have found a putative global minimum (GM), we perform an “atom-exchange” routine (a modified Basin Hopping Monte Carlo, in collaboration with Professor Alessandro Fortunelli and Dr. Giovanni Barcaro, CNR-Pisa).

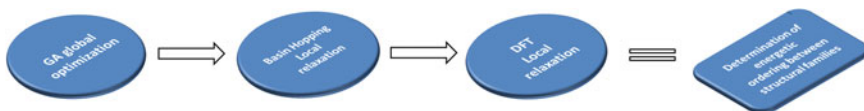


Fig. 2.6 Schematic representation of our *combined approach*

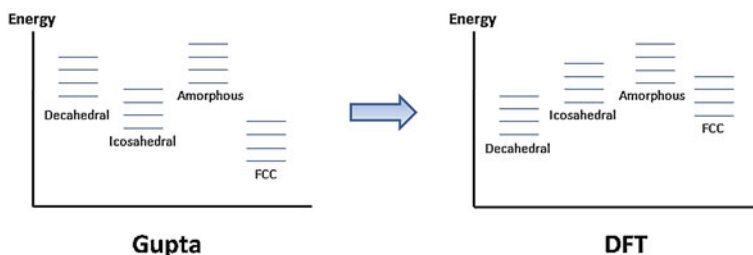


Fig. 2.7 *Left* putative GM *structural families* found at the Gupta level of theory. The energy orderings are modified after performing high-level DFT calculations *right*

This allows us to corroborate, at the Gupta level, the *chemical ordering* of the structure (i.e. the way in which atoms segregate to cluster surface sites). Once we have located a variety of putative GM structures (as well as high-energy isomers) for different bimetallic systems, we proceed to construct a database of structures (varying from crystalline fcc-type structures, to decahedral, icosahedral and amorphous type, *structural families*); and we place them in competition at the high level of theory, by carrying out DFT local-relaxations on these structures (see Fig. 2.7) [36, 38, 39].

In contrast to the search of the empirical potential (EP) potential energy surface using the GA method, we cannot guarantee that our combined EP/DFT approach will be equally successful in the search of the GM at the DFT level. For this reason, the expressions “putative GM” or “lowest-energy structure” are used when discussing the results of DFT calculations.

## 2.4 Energetic Analysis

In order to analyse cluster stability, some energetic quantities need to be defined. At the Gupta potential level of theory, the *binding energy* per atom of a cluster ( $E_b^{\text{Gupta}}$ ), can be calculated as:

$$E_b^{\text{Gupta}} = -\frac{V_{\text{clus}}}{N} \quad (2.29)$$

where  $V_{\text{clus}}$  is the total potential energy of the cluster (pure metal or bimetallic) and  $N$  is the total number of atoms in the cluster. In our work, positive values of  $E_b^{\text{Gupta}}$  indicate stable cluster atomic configurations (i.e. lower  $E_b^{\text{Gupta}}$  values would indicate less favourable atomic arrangements). Another criterion for determining relative stability (both at the Gupta and DFT level) is the *second difference in binding energy*,  $\Delta_2 E_b(N)$ . This quantity is used in pure clusters in order to compare the relative stability of a cluster of size  $N$ , with respect to its neighbours:

$$\Delta_2 E_b(N) = 2E_b(N) - E_b(N-1) - E_b(N+1) \quad (2.30)$$

In the case of mixed clusters, Eq. 2.30 can be defined as follows:

$$\Delta_2 E_b(A_m B_n) = E_b(A_{m+1} B_{n-1}) + E_b(A_{m-1} B_{n+1}) - 2E_b(A_m B_n) \quad (2.31)$$

where peaks in both  $\Delta_2 E_b(N)$  and  $\Delta_2 E_b(A_m B_n)$  often coincide with discontinuities in the mass spectra [40].

Another useful quantity at the Gupta level is the *excess energy* (i.e. the *mixing energy*)  $\Delta_N^{\text{Gupta}}$  defined for clusters of fixed size but different composition [41]:

$$\Delta_N^{\text{Gupta}} = E_N^{\text{Gupta}}(A_m B_n) - m \frac{E_N^{\text{Gupta}}(A_N)}{N} - n \frac{E_N^{\text{Gupta}}(B_N)}{N} \quad (2.32)$$

where  $E_N^{\text{Gupta}}(A_m B_n)$  represents the total energy of a given cluster (e.g. all possible compositions for  $N$ -atom: Pd–Pt, Ag–Pt, Pd–Au and Ag–Au clusters) calculated at the Gupta level and  $E_N^{\text{Gupta}}(A_N)$  and  $E_N^{\text{Gupta}}(B_N)$  represent the total energies of the GM of the pure metal clusters (i.e.  $\text{Pt}_N$ ,  $\text{Ag}_N$ ,  $\text{Pd}_N$  and  $\text{Au}_N$ ).  $\Delta_N^{\text{Gupta}}$  quantifies the degree of mixing (the energy associated with alloying) between the two different metals. The most negative values of  $\Delta_N^{\text{Gupta}}$  represent those compositions at which mixing is most favourable, and thus, the more stable clusters.

In order to analyse trends in chemical order as a function of size and composition (See Chap. 7), it is convenient to define an order parameter with the following characteristics: positive when phase separation (segregation) takes place, close to zero when disordered mixing occurs, and negative when mixing and layer-like structure co-exist. The chemical order parameter  $\sigma$  is defined as:

$$\sigma = \frac{N_{\text{Pd-Pd}} + N_{\text{Au-Au}} - N_{\text{Pd-Au}}}{N_{\text{Pd-Pd}} + N_{\text{Au-Au}} + N_{\text{Pd-Au}}} \quad (2.33)$$

where  $N_{ij}$  (with  $i, j = \text{Pd, Au}$ ) is the number of nearest neighbour  $i-j$  bonds. An order parameter of this type has proven to be useful in the description of short range order in binary bulk alloys and surfaces [42].

The *DFT binding energies* ( $E_b^{\text{DFT}}$ ) for  $N$ -atom pure metal clusters can be calculated as the difference (per atom) between the total electronic energy of the cluster ( $E_{\text{total}}^{\text{DFT}}(A_N)$ ) and  $N$  times the energy of a single atom  $E_{\text{atom}}^{\text{DFT}}(A)$ :

$$E_b^{\text{DFT}} = -\frac{1}{N} [E_{\text{total}}^{\text{DFT}}(A_N) - N \cdot E_{\text{total}}^{\text{DFT}}(A)] \quad (2.34)$$

For bimetallic clusters,  $E_b^{\text{DFT}}$  is calculated using a similar expression:

$$E_b^{\text{DFT}} = -\frac{1}{N} [E_{\text{total}}^{\text{DFT}}(A_m B_n) - m \cdot E_{\text{atom}}^{\text{DFT}}(A) - n \cdot E_{\text{atom}}^{\text{DFT}}(B)] \quad (2.35)$$

The excess energy  $\Delta_N^{\text{DFT}}$ , can also be defined at the DFT level as follows:

$$\Delta_N^{\text{DFT}} = E_N^{\text{DFT}}(A_m B_n) - m E_{A_N}^{\text{DFT}} - n E_{B_N}^{\text{DFT}} \quad (2.36)$$

where  $E_N^{\text{DFT}}(A_m B_n)$  is the total electronic energy of the cluster, with size  $N$  and composition  $(A_m B_n)$ , and  $E_{A_N}^{\text{DFT}}$  and  $E_{B_N}^{\text{DFT}}$  are the total electronic energies of the GM of the pure metal clusters  $A_N$  and  $B_N$ , respectively.

## References

1. D.J. Wales, *Energy Landscapes, with Applications to Clusters, Biomolecules and Glasses* (Cambridge University Press, Cambridge, 2003)
2. R.P. Gupta, Phys. Rev. B **23**, 6265 (1981)
3. F. Cleri, V. Rosato, Phys. Rev. B **48**, 22 (1993)
4. L.H. Thomas, Proc. Camb. Phil. Soc. **23**, 542 (1927)
5. E. Fermi, Z. Phys. **48**, 73 (1928)
6. R.G. Parr, W. Yang, *Density-Functional Theory of Atoms and Molecules* (Oxford University Press, Oxford, 1989)
7. M. Finnis, *Interatomic Forces in Condensed Matter* (Oxford University Press, Oxford, 2003)
8. P.W. Atkins, R.S. Friedman, *Molecular Quantum Mechanics*, 3rd edn. (Oxford University Press, Oxford, 1997)
9. P. Hohenberg, W. Kohn, Phys. Rev. **136**(3B), B864
10. W. Kohn, L.S. Sham, Phys. Rev. **140**(4A), A1133 (1965)
11. W. Kohn, Rev. Mod. Phys. **71**(5), 1253 (1999)
12. D.M. Ceperley, B.J. Alder, Phys. Rev. Lett. **45**, 566 (1980)
13. A. Khein, D.J. Singh, C.J. Umrigar, Phys. Rev. B **51**, 4105 (1995)
14. J.P. Perdew, Y. Wang, Phys. Rev. B **33**, 8800 (1986)
15. J.P. Perdew, J.A. Chevary, S.H. Vosko, K.A. Jackson, M.R. Pederson, D.J. Singh, C. Fiolhaus, Phys. Rev. B **46**, 6671 (1992)
16. F. Jensen, *Introduction to Computational Chemistry* (Springer, Berlin, 1999)
17. R.A. Kendall, E. Aprà, D.E. Bernholdt, E.J. Bylaska, M. Dupuis, G.I. Fann, R.J. Harrison, J. Ju, J.A. Nichols, J. Nieplocha, T.P. Straatsma, T.L. Windus, A.T. Wong, Comput. Phys. Commun. **128**, 260 (2000)
18. J.P. Perdew, K. Burke, M. Ernzerhof, Phys. Rev. Lett. **77**, 3865 (1996)
19. E. Aprà, A. Fortunelli, J. Mol. Struct. (Theochem) **501**, 251 (2000)
20. J. Paier, M. Marsman, G. Kresse, J. Chem. Phys. **127**, 024103 (2007)
21. A. Schäfer, C. Huber, R. Ahlrichs, J. Chem. Phys. **100**, 5829 (1994)
22. See: <ftp://ftp.chemie.uni-karlsruhe.de/pub/basen/>
23. D. Andrae, U. Haeussermann, M. Dolg, H. Stoll, H. Preuss, Theor. Chim. Acta. **77**, 123 (1990)
24. F. Weigend, M. Haser, H. Patzel, R. Ahlrichs, Chem. Phys. Lett. **294**, 143 (1998)
25. E. Aprà, A. Fortunelli, J. Phys. Chem. A **107**, 2934 (2003)

26. S. Baroni, A. Del Corso, S. de Gironcoli, P. Giannozzi, <http://www.pwscf.org>
27. G. Barcaro, F. Sedona, A. Fortunelli, G. Granozzi, *J. Phys. Chem. C* **111**, 6095 (2007)
28. D. Lawrence, *Handbook of Genetic Algorithms*. ed. Van Nostrand Reinhold, New York (1991)
29. J. Holland, *Adaptation in Natural and Artificial Systems*. Springer, Berlin (1975)
30. R.L. Johnston, *Dalton Trans.* 4193 (2003)
31. B. Hartke, *Applications of Evolutionary Computation in Chemistry*, in R.L. Johnston, (Springer, Berlin, 2004)
32. E. Schroeder-Reiter, F. Pérez-Willard, U. Zeile, G. Wanner, *J. Struct. Bio.* **165**, 97 (2009)
33. R.H. Byrd, P. Lu, J. Nocedal, Zhu C, *J. Scient. Comp.* **5**, 1190 (1995)
34. J.P.K. Doye, D.J. Wales, *J. Phys. Chem. A* **101**, 5111 (1997)
35. L.O. Paz-Borbón, T.V. Mortimer-Jones, R.L. Johnston, A. Posada-Amarillas, G. Barcaro, A. Fortunelli, *Phys. Chem. Chem. Phys.* **9**, 5202 (2007)
36. R. Ferrando, R.L. Johnston, A. Fortunelli, *Phys. Chem. Chem. Phys.* **10**, 640 (2008)
37. N.T. Wilson, R.L. Johnston, *J. Mater. Chem.* **12**, 2913 (2002)
38. L.O. Paz-Borbón, R.L. Johnston, G. Barcaro, A. Fortunelli, *J. Chem. Phys.* **128**, 134517 (2008)
39. L.O. Paz-Borbón, R.L. Johnston, G. Barcaro, A. Fortunelli, *J. Phys. Chem. C* **111**, 2936 (2007)
40. W.D. Knight, K. Clemenger, W.A. de Heer, W.A. Saunders, M.Y. Chou, M.L. Cohen, *Phys. Rev. Lett.* **52**, 2141 (1984)
41. R. Ferrando, R.L. Johnston, J. Jellinek, *Chem. Rev.* **108**, 845 (2008)
42. F. Aguilera-Granja, A. Vega, J. Rogan, X. Andrade, G. García, *Phys. Rev. B.* **74**, 224405 (2006)